siRNA-based spherical nucleic acids reverse impaired wound healing in diabetic mice by ganglioside GM3 synthase knockdown

Pratik S. Randeria[a,b], Mark A. Seeger[c], Xiao-Qi Wang[c], Heather Wilson[c], Desmond Shipp[c], Chad A. Mirkin[a,b,d,1], and Amy S. Paller[c,1]

Departments of [a]Biomedical Engineering and [d]Chemistry and [b]International Institute for Nanotechnology, Northwestern University, Evanston, IL 60208; and [c]Department of Dermatology, Feinberg School of Medicine, Northwestern University, Chicago, IL 60611

Contributed by Chad A. Mirkin, March 25, 2015 (sent for review February 13, 2015; reviewed by Dean Ho and Wei Li)

Spherical nucleic acid (SNA) gold nanoparticle conjugates (13-nm-diameter gold cores functionalized with densely packed and highly oriented nucleic acids) dispersed in Aquaphor have been shown to penetrate the epidermal barrier of both intact mouse and human skin, enter keratinocytes, and efficiently down-regulate gene targets. ganglioside-monosialic acid 3 synthase (GM3S) is a known target that is overexpressed in diabetic mice and responsible for causing insulin resistance and impeding wound healing. GM3S SNAs increase keratinocyte migration and proliferation as well as insulin and insulin-like growth factor-1 (IGF1) receptor activation under both normo- and hyperglycemic conditions. The topical application of GM3S SNAs (50 nM) to splinted 6-mm-diameter full-thickness wounds in diet-induced obese diabetic mice decreases local GM3S expression by >80% at the wound edge through an siRNA pathway and fully heals wounds clinically and histologically within 12 d, whereas control-treated wounds are only 50% closed. Granulation tissue area, vascularity, and IGF1 and EGF receptor phosphorylation are increased in GM3S SNA-treated wounds. These data capitalize on the unique ability of SNAs to naturally penetrate the skin and enter keratinocytes without the need for transfection agents. Moreover, the data further validate GM3 as a mediator of the delayed wound healing in type 2 diabetes and support regional GM3 depletion as a promising therapeutic direction.

SNA | nanoparticle | siRNA | GM3 synthase | diabetic wound healing

Of 27 million Americans diagnosed with type 2 diabetes (T2D), more than 6 million have chronic, nonhealing skin wounds, particularly on the plantar surface, leading to secondary bacterial infection and costing the healthcare system more than $25 billion (1, 2). In 2010 alone, more than 70,000 individuals in the United States with T2D underwent amputation (3). Improved understanding of diabetic wound pathology and new interventions for impaired wound healing are needed.

Ganglioside-monosialic acid 3 (GM3), the predominant sialylated glycosphingolipid in skin, has recently been recognized to be a critical mediator of insulin resistance (4–12). Indeed, we have recently shown three- and fourfold more GM3 synthase (GM3S; also known as SAT-I or ST3Gal-V), which is required for the synthesis of GM3, in diabetic human plantar skin than in site- and age-matched control skin (4). Similarly, skin samples from the backs of diet-induced obese (DIO) and ob/ob mouse diabetic models show increased GM3S mRNA expression and GM3 levels. Knockout (KO) of GM3S improves the insulin resistance induced by a high-fat diet in mouse adipose tissue, muscle (5), and as recently shown, skin of DIO T2D mice, reversing the wound-healing impairment of T2D (4). The acceleration of wound healing by GM3S KO and GM3 depletion in mouse skin is associated with increased epidermal cell migration and proliferation as well as activation of the epidermal insulin-like growth factor-1 receptor (IGF1R) in vivo (4). Isolated cultured mouse $GM3S^{-/-}$ keratinocytes (KCs) migrate and proliferate more rapidly than $GM3S^{+/+}$ WT littermate KCs, resist the inhibition of migration and proliferation induced by increased ambient glucose (simulating hyperglycemia), and show activation of IGF1R and insulin receptor. These findings show that accelerated wound healing, at least in part, is reflected by a direct action of GM3S suppression on wound area KCs and suggest that a topical intervention to knock down GM3S in skin might accelerate the impaired wound healing in T2D.

Spherical nucleic acids (SNAs; structures made by chemically modifying gold nanoparticles with dense layers of highly oriented oligonucleotides) are an emerging class of gene regulation entities that show promise for both antisense and RNAi pathways (13, 14). These structures can be rapidly synthesized from readily available nucleic acid and nanoparticle precursors and exhibit attractive biological properties, including nuclease resistance (15), the ability to rapidly enter cells through scavenger receptor-mediated endocytosis (16), and the ability to effect gene knockdown in several in vivo models without apparent cellular toxicity or off-target effects (17, 18). Previous studies have shown that SNAs, dispersed in a common moisturizer, can traverse the epidermal barrier in C57BL/6 mouse models and human skin equivalents and can be used to specifically down-regulate EGF receptor (EGFR) (17). Taken together, these properties point toward the potential for developing new topically applied gene regulation therapies for skin diseases. Herein, we report the development of siRNA-based GM3S SNA, which efficiently and specifically

Significance

Diabetic patients often suffer from impaired wound healing, which can develop into nonhealing diabetic ulcers, facilitate bacterial infections, and necessitate amputation. Current strategies for treatment have failed to achieve the anticipated efficacy and do not address the fundamental molecular abnormalities that prevent efficient wound closure. In this work, we introduce a previously unidentified approach to treating diabetic wound healing by using topically delivered spherical nucleic acids to effect the knockdown of ganglioside-monosialic acid 3 (GM3) synthase, a mediator of impaired wound healing, in type 2 diabetic mice. In addition to laying the groundwork for developing a therapy for a debilitating condition, this work also validates the critical role of GM3 in diabetic wound healing.

Author contributions: P.S.R., M.A.S., C.A.M., and A.S.P. designed research; P.S.R., M.A.S., X.-Q.W., H.W., and D.S. performed research; P.S.R., M.A.S., X.-Q.W., C.A.M., and A.S.P. analyzed data; and P.S.R., M.A.S., X.-Q.W., C.A.M., and A.S.P. wrote the paper.

Reviewers: D.H., University of California, Los Angeles; and W.L., University of Southern California.

Conflict of interest statement: C.A.M. is a cofounder of Aurasense Therapeutics, LLC, and A.S.P. is on the advisory board of Aurasense Therapeutics, LLC.

[1]To whom correspondence may be addressed. Email: chadnano@northwestern.edu or apaller@northwestern.edu.

This article contains supporting information online at www.pnas.org/lookup/suppl/doi:10.1073/pnas.1505951112/-/DCSupplemental.

knocks down the expression of GM3S mRNA and protein in cultured KCs as well as both intact and wounded mouse skin. GM3S SNA treatment promotes KC migration into the wound bed, increases IGF1R and EGFR phosphorylation, and accelerates wound closure in T2D mice. This work constitutes an innovative approach to diabetic wound healing and represents the first topical therapeutic application, to our knowledge, of SNA nanotechnology. Moreover, it lays the groundwork for developing SNA approaches to treatment of many of the more than 200 skin-related disorders with a known genetic basis (19).

Results

GM3S SNA Synthesis and Characterization. After initially screening GM3S-targeting oligomers (Fig. S1 and Table S1) through conventional DharmaFECT1-mediated nucleic acid transfection, the five best siRNAs with knockdown of >70% were conjugated to gold nanoparticles to make SNAs. Of these, two SNAs had oligonucleotide sequences with perfect homology between mouse and human GM3S and showed >75% knockdown of both mouse and human GM3S. The more effective of these two, SNA 804 (GM3S SNA), was chosen for all therapeutic studies (see below).

The SNAs had a 13 ± 1-nm-diameter gold nanoparticle core to which the sense strand of the duplexed siRNA was attached by a propylthiol linkage. The remaining surface of the gold was filled with thiolated oligoethylene glycol, which functions as a passivating agent and provides additional stability to the particle in biological solutions (Fig. 1*A*) (13, 14). Dynamic light scattering and transmission EM analyses indicated that the GM3S SNA had an average hydrodynamic diameter of 28 ± 3 nm and remained dispersed in solution (Fig. 1*B*). The GM3S SNA had an average siRNA loading of 40 ± 5 siRNA duplexes per particle, and each siRNA duplex on the SNA remained hybridized and stable in solution for more than 75 d (Fig. 1*C*). Taken together, these data indicate that GM3S SNA nanoparticles are sufficiently robust, stable, and homogenous for testing in in vitro and in vivo applications.

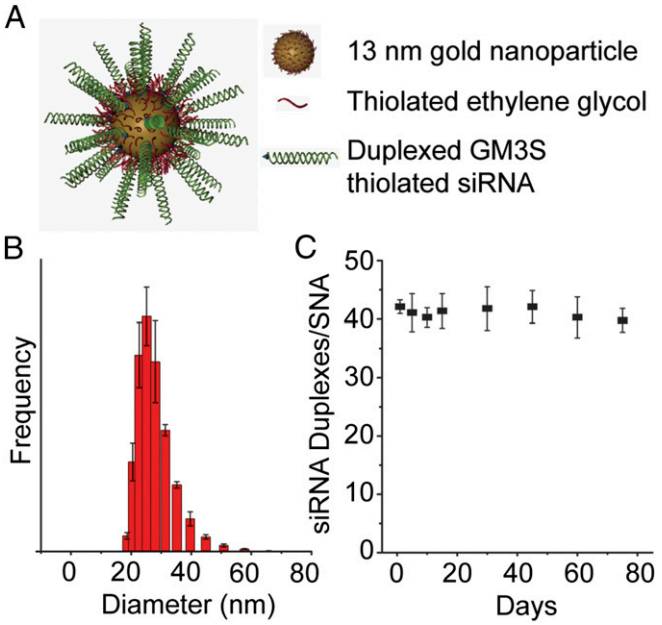

Fig. 1. SNA depiction and characterization. (*A*) SNAs are 13-nm gold cores densely functionalized with highly oriented, thiolated siRNA duplexes that target GM3S. The SNA surface is passivated with oligoethylene glycol for colloidal stability. (*B*) Dynamic light scattering confirms the hydrodynamic diameter to be ∼32 nm. (*C*) Approximately 40 siRNA duplexes are anchored to each gold nanoparticle, and quantification over 75 d shows that the number of full siRNA duplexes remains statistically identical during that time period. Stability data are represented as means ± SDs.

In contrast with the nontreated (NT) and nonsense (NS) SNA-treated immortalized mouse KCs (mKCs), GM3S SNA reduced both GM3S mRNA and protein by >80% at a concentration of 5 nM (based on the gold particle concentration and equivalent to 200 nM free siRNA, because ∼40 duplex siRNAs surround the central nanoparticle). Knockdown occurred in a dose-dependent manner (Fig. 2 *A* and *B*). In primary epidermal mKCs, 2.5 nM GM3S SNA knocked down GM3S mRNA and protein by 79% and 88%, respectively. Confocal immunofluorescence of immortalized mouse (Fig. 2*C*) and human KCs (Fig. S2) with anti-GM3 antibody confirmed almost complete elimination of GM3 ganglioside expression after 72 h of GM3S SNA treatment. GM3S SNA was nontoxic to mKCs at all concentrations tested, which was assessed by a trypan blue exclusion cell viability assay, including at siRNA concentrations toxic to >95% of mKCs when treated with free siRNA delivered with the DharmaFECT1 transfection reagent (Fig. 2*D*).

GM3S SNA Stimulates KC Migration and Proliferation in Vitro. The functional effect of knocking down GM3S in primary mKCs growing in serum-free CnT07 medium in vitro, including compared with GM3S$^{-/-}$ primary mKCs (4), was studied using scratch (in vitro wound healing) (Fig. 2*E*) and water-soluble tetrazolium proliferation assays (Fig. 2*F*) (20). In previous studies, we showed that GM3-depleted KCs have increased migration and proliferation, including when incubated in excess glucose, which suppress migration and proliferation in GM3S$^{+/+}$ KCs (4); 60 h after the scratch, GM3S SNA-treated wounds were completely closed in hyperglycemic conditions (Fig. 2*E*) and almost closed in normoglycemic medium (Fig. S3) but remained >50% open in NT and NS SNA-treated scratch wounds. After 3 ($P < 0.05$) and 5 d ($P < 0.001$) in culture, mKCs treated with 2 nM GM3S SNA showed greater proliferation than controls at a rate comparable with that of GM3S$^{-/-}$ mKCs (Fig. 2*F*). These studies suggest that GM3S reduction by GM3S SNA functionally recapitulates the effect of GM3S KO on KC migration and proliferation.

GM3S SNA Depletes GM3S in Vivo Through the RNAi Pathway. The efficacy of GM3S SNA for GM3S knockdown and improved wound healing in vivo was then tested in the C57BL/6 DIO T2D mouse model, which resembles diet-induced T2D in humans and has impaired wound healing (4, 21). All mice weighed at least 39 g at baseline (mean = 43 ± 2.13 g) and exhibited high mean fasting glucose and impaired glucose uptake (Fig. S4). Weights were maintained throughout the wound-healing studies (Fig. S4). Two circular full-thickness 6-mm-diameter wounds were made on the backs of diabetic mice, and silicone splints were affixed to the skin surrounding the wound to minimize the contraction-mediated wound healing and maximize reepithelialization (22). Wound edges were treated every other day with NT (control), NS SNA (NS control; 50 nM), GM3S SNA (50 nM), or free GM3S siRNA (2 μM; equivalent to the siRNA content in 50 nM SNA; harvested only at 6 and 12 d) in a 1:1 wt/wt mixture of Aquaphor, a commercially available moisturizer, in PBS. GM3S SNA-treated wound edge skin showed a 70–80% decrease in GM3S mRNA by 3 d (two treatments) and protein expression by 6 d (three treatments) and beyond after wounding and initiating GM3S SNA ($P < 0.01$) relative to the NS SNA-treated wounds (Fig. 3 *A* and *B*). Free GM3S siRNA did not lead to a decrease in GM3 at 6 or 12 d; 5′-RNA ligase-mediated (5′-RLM) -RACE showed cDNA fragment lengths in GM3S SNA-treated wound border skin consistent with RNAi-mediated cleavage of GM3S mRNA (Fig. 3*C*).

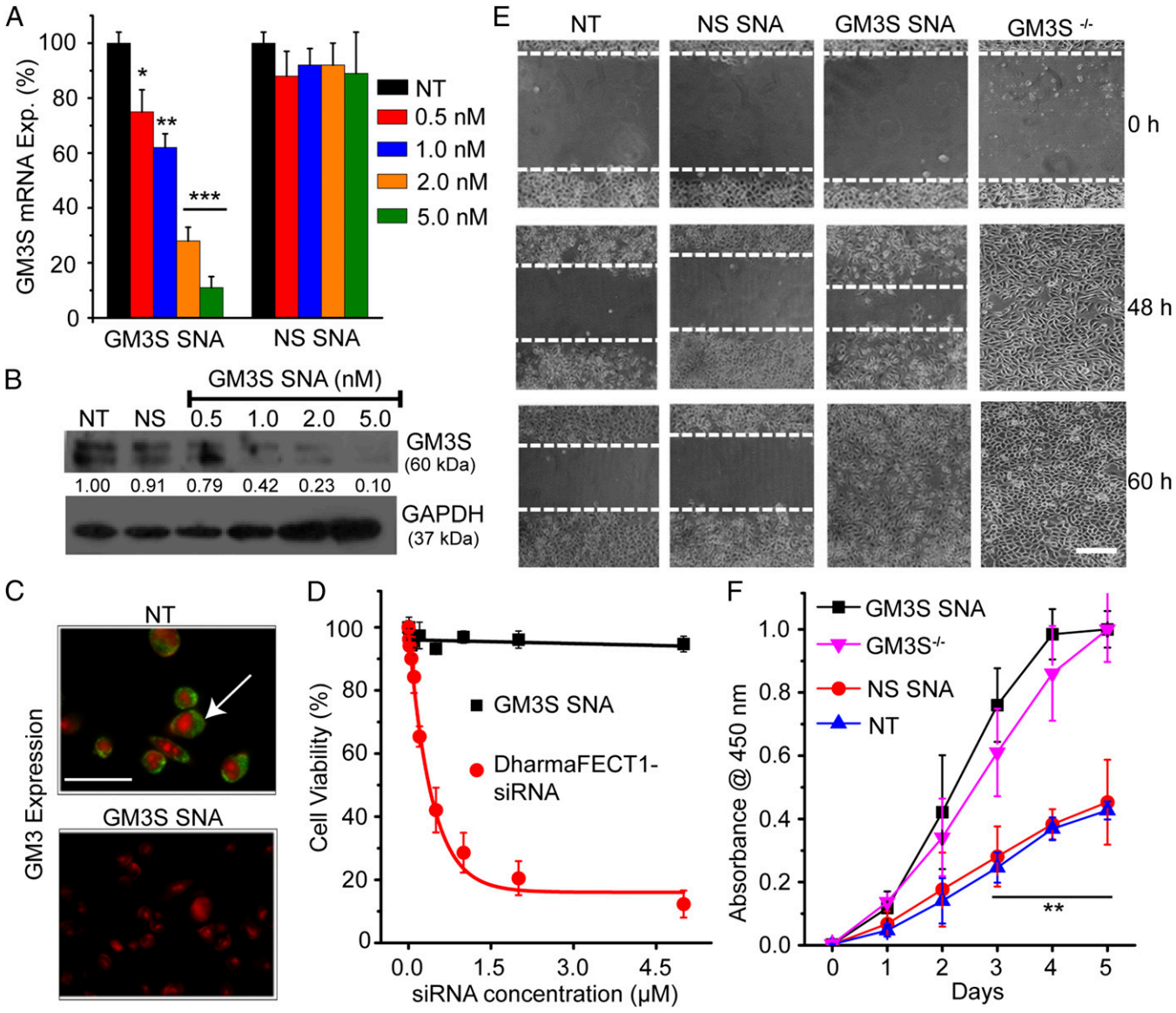

Fig. 2. In vitro characterization of GM3S SNA. (*A*) GM3S mRNA and (*B*) protein expression as quantified by RT-PCR and Western blotting after GM3S SNA and NS SNA (0.5, 1.0, 2.0, and 5.0 nM) were incubated with immortalized mKCs in complete medium. GM3S SNA led to a dose-dependent decrease in GM3S mRNA and protein expression as low as 20% of that of control-treated cells. A significant reduction in GM3S mRNA from NS SNA-treated controls was noted with as little as 0.5 nM GM3S SNA. (*C*) Confocal immunofluorescence shows elimination of GM3 in KCs treated with (*Lower*) GM3S SNA relative to (*Upper*) NT (arrow; green, GM3; red, propidium iodide-stained nuclei). (Scale bar: 50 μm.) (*D*) Trypan blue exclusion assay showed excellent cell viability after 48 h of treatment with GM3S SNA treatment vs. the identical siRNA sequence coupled with DharmaFECT1 transfection agent. (*E*) In vitro wound closure (scratch assay) of primary mKCs in serum-free medium with excess glucose (total of 18 mM) were pretreated for 48 h with GM3S SNA, NS SNA, or NT, scratched, and monitored for wound closure. mKCs from GM3S KO mice ($GM3S^{-/-}$) were studied as a positive control. (Scale bar: 120 μm.) (*F*) In water-soluble tetrazolium-1 assays, GM3S SNAs increased proliferation of primary mKCs within 3 d with a course similar to that of $GM3S^{-/-}$ mKCs. All data are represented as means ± SDs. All studies were performed in triplicate at least three times. $*P < 0.05$; $**P < 0.01$; $***P < 0.001$.

GM3S SNA Normalizes Diabetes-Induced Wound-Healing Impairment. Treatment with 50 nM GM3S SNAs applied every other day accelerated wound closure in the DIO diabetic mice relative to control wounds treated with vehicle, NS SNA, or free GM3S siRNA (Fig. 4 *A–D*). Acceleration of wound healing, as visualized clinically, was observed within 4 d (two treatments; $P < 0.01$). The GM3S SNA-treated wounds were clinically healed by 12 d after wounding, whereas control-treated wounds remained open for an average of 18 d ($P < 0.001$) (Fig. 4 *A* and *B* and Fig. S5). Wound closure was confirmed histologically through measurement of the epidermal gap. Reduction in epidermal gap relative to control-treated wounds was first observed by 6 d (three applications) after initiation of GM3S siRNA SNA treatment, by which time the GM3S SNA-treated wounds had an epidermal gap of 23% of that of the control wounds ($P < 0.001$). Reepithelialization was complete in GM3S SNA-treated wounds by an average of 12 d, whereas control-treated wounds remained >50% open at this time point (Fig. 4*C*). Granulation tissue area was increased nearly fourfold by the time of closure of GM3S SNA-treated mice compared with controls (Fig. 4*E*, *Left*) ($P < 0.01$). Dermal $CD31^+$ cells, a marker of wound vascularity, were increased almost twofold in the same wounds compared with NS and NT controls ($P < 0.05$) (Fig. 4*E*, *Right*).

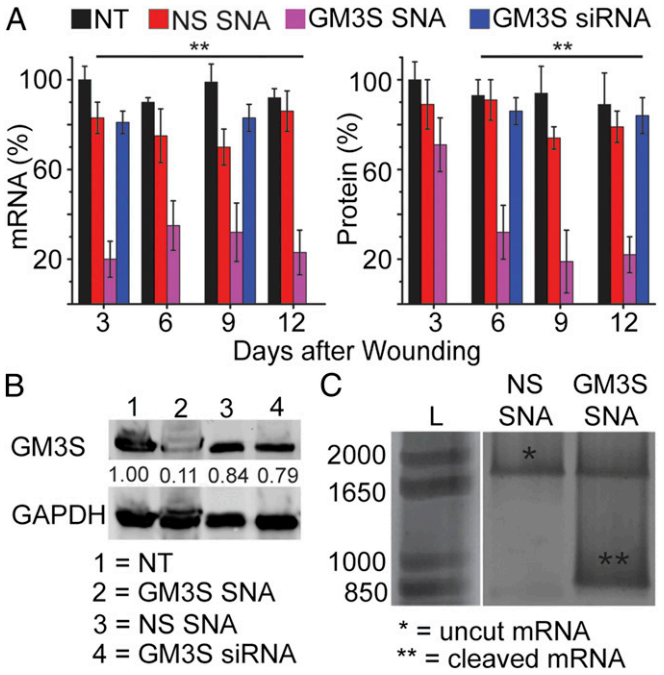

Fig. 3. Topically applied GM3S SNA down-regulates cutaneous GM3S levels in DIO mice. (*A*) RT-PCR and Western blotting were performed on mouse skin harvested 3, 6, 9, and 12 d after wounding and for free GM3S siRNA, at 6 and 12 d. Topically applied 50 nM GM3S SNA resulted in 70–80% knockdown of GM3S mRNA ($P < 0.01$) within the first two applications (3 d) and GM3S protein by 6 d (three applications; $P < 0.01$) compared with all controls, including free GM3S siRNA. All data are represented as means ± SDs. $^{**}P < 0.01$. (*B*) A representative Western blot shows an 89% reduction in GM3S protein after five GM3S SNA treatments. (*C*) For 5′-RLM-RACE analysis, total mRNA from treated mouse skin was extracted, GM3S mRNA was reverse-transcribed to cDNA, and the cDNA was amplified by PCR. Gel electrophoresis of amplified cDNA shows predominantly a shorter band in mice treated with GM3S SNA vs. the longer band primarily in mice treated with NS SNA, consistent with RNAi-mediated mRNA cleavage. L refers to the DNA ladder, with molecular weights annotated. All studies were performed three to four times on at least eight wounds per group per run. *Longer band; **shorter band.

GM3S SNA Activates EGFR and IGF1R in Wounded Diabetic Skin. In addition to the stimulatory effect of GM3 depletion on insulin receptor/IGF1R activation, our past studies have shown that GM3 inhibits activation of EGFR in normal and neoplastic KCs and that decreased functional GM3 increases EGFR phosphorylation (20). Immunoblotting using whole-protein lysates from skin at the wound edge showed increases in the phosphorylation but not the total protein of IGF1R (Fig. 4*F*) and EGFR (Fig. 4*G*). Immunohistochemical staining similarly showed increased expression of phosphorylated (p)-IGF1R (Fig. S6) and p-EGFR in GM3S SNA-treated epidermis at the wound edge.

GM3S SNAs Do Not Cause Obvious Evidence of Tissue Toxicity. Treatment with GM3S SNAs did not lead to weight loss or abnormal mouse behavior, and it was not associated with skin discoloration, inflammation, thickening, or atrophy. Similarly, the epidermis and the dermis in the treated sections did not show evidence of increased inflammation or cell apoptosis relative to wounds in diabetic mouse controls. In mice with 12-d wounds (and seven treatments), organs were evaluated for evidence of SNA accumulation after termination using inductively coupled plasma MS; 87% of all detected SNAs (from either GM3S SNA or NS SNA) had accumulated in the skin. Less than 1% of the topical dose was found in the spleen, trace amounts were found in the regional lymph nodes and liver, and none was found in the kidney or lungs (Fig. S7).

Discussion

We have engineered an RNAi-based gene regulator, GM3S SNA, that significantly accelerates KC migration and proliferation in mouse diabetic wounds by depleting ganglioside GM3, a recently identified mediator of insulin resistance (4). SNA constructs are able to penetrate the stratum corneum of intact skin, rapidly enter epidermal and dermal cells, and knock down epidermal targets (17). In contrast to SNAs, other topical siRNA-based therapies require epidermal disruption by physical [e.g., injection, tape stripping (23), laser, or ultrasound] or chemical (e.g., conjugation to peptides or lipoplexes or incorporation into other types of nanoparticle structures, lentiviruses, or gels) means for RNAi penetration through the epidermal barrier and into KCs (24–31). siRNA SNAs are unique, highly anionic constructs that do not require additional chemical modifications to facilitate transportation through the stratum corneum or entry into cells. The SNA constructs have been shown to be highly efficacious and do not show apparent toxicity in in vivo gene regulation applications (17, 18), including in this study with diabetic mice. Despite the absence of an epidermal barrier at the wound itself, the failure of free GM3S siRNA to improve wound healing suggests that the ability of GM3S SNA to traverse the epidermal barrier at the wound edge and knock down its target plays an important role in accelerating regional KC migration and proliferation.

Wound healing is a complex process, requiring the integration of a diverse set of cellular chemical, molecular, and mechanical signals, which are perturbed in T2D. KC migration into the wound site is a critical step in wound closure but has received relatively little attention in diabetic wounds. Among the most potent stimulants of KC migration and proliferation are EGFR ligands and insulin-like growth factor-1, which activates IGF1R and, to a lesser extent, the insulin receptor (32–34). Ligands for EGFR and IGF1R have additive effects on wound reepithelialization, influencing different signaling pathways that lead to accelerated KC migration (35). Our studies further verify the key role of IGF1R and EGFR phosphorylation in wound healing, showing suppression in epidermal p-IGF1R and p-EGFR in diabetic mouse epidermis but reversal of that suppression with GM3S SNA intervention and accelerated wound closure. It should be noted that the increase in the activation of both receptors was because of phosphorylation alone and not because of an increase in receptor expression. In this study, we focused on two important growth factor receptors in epidermis, EGFR and IGF1R, but several other growth factors have been noted to impact KC migration. The shown acceleration in migration in serum-free medium provides an opportunity to screen for activation of other growth factor receptors by GM3 depletion.

The impact of GM3S SNA parallels the effect of GM3S KO in the wounded DIO $GM3S^{-/-}$ mouse, which resists the development of insulin resistance and wound-healing impairment, despite diet-induced obesity (4). Much attention has focused on vascular abnormalities in the pathogenesis of the delayed wound healing in diabetes (36–38). The observation that GM3S SNA treatment almost doubles $CD31^{+}$ cells in the wounds provides evidence that the regional suppression of GM3 synthesis may play a role in stimulating angiogenesis as well and supports the previously shown inhibition of VEGF receptor-2 activation and angiogenesis by GM3 (36).

The work conducted in this study is important because it (*i*) confirms the key role of GM3 as a critical mediator of insulin resistance and establishes the depletion of GM3 levels as a treatment modality for diabetic ulcers, (*ii*) represents a previously unidentified topically applied, RNAi-based strategy to accelerate wound closure in mice, and (*iii*) provides the blueprint for a platform that can be used to treat any skin-related

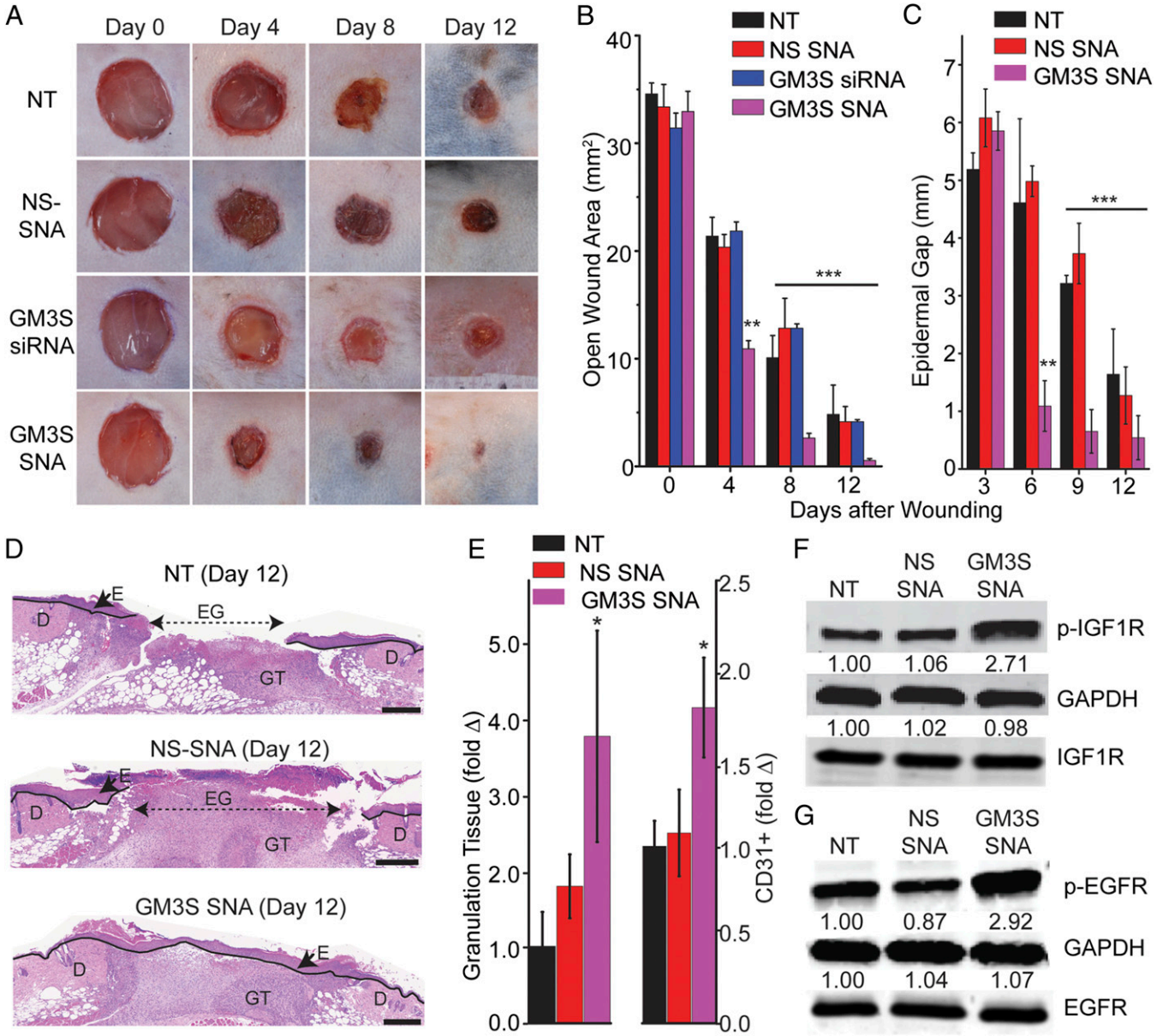

Fig. 4. Topical application of GM3S SNA prevents the delayed wound healing in the DIO mouse. (*A*) Representative clinical images of wounds. (*B*) Computerized measurements of the open wound area were performed using ImageJ ($n = 8$ wounds per day and treatment group). $^{**}P < 0.01$; $^{***}P < 0.001$. (*C*) Epidermal gap (the maximum distance between KCs at the leading wound edges) was measured by computerized morphometry. $^{**}P < 0.01$; $^{***}P < 0.001$. (*D*) Representative histologic images of NT and NS SNA- and GM3S SNA-treated wounds at day 12. D, dermis; E, epidermis; EG, epidermal gap; GT, granulation tissue. (Scale bar: 500 μm.) (*E*, *Left*) Granulation tissue area and (*E*, *Right*) vascularity ($CD31^+$ staining) were measured by computerized morphometry. At least six sections were analyzed for each treatment group ($n = 6$). Data shown are means ± SEs. $^{*}P < 0.05$ for comparison of NT, NS SNA-treated, and free GM3S siRNA-treated mice with GM3S SNA-treated mice. Expression of phosphorylation of (*F*) IGF1R and (*G*) EGFR in wound edges of skin.

disease with a genetic basis. The results from this investigation are an exciting first step toward the development of oligonucleotide-based therapeutics for skin disorders, paving the way for additional studies of SNA efficacy in more complex animal models.

Methods

SNA Synthesis and Characterization. Thirteen siRNA duplexes targeting homologous sequences in murine and human GM3S mRNA were synthesized and introduced into immortalized mKCs using the DharmaFECT1 transfection reagent (GE Life Sciences) and screened for GM3S mRNA and protein knockdown (Fig. S1). The most effective siRNA sequences were densely conjugated onto gold nanoparticles to make GM3S-targeting SNAs (details in *SI Text, SNA Synthesis and Characterization*). Dynamic light scattering (Malvern) and transmission EM (Hitachi 2300) were used to characterize the hydrodynamic diameter. A Quant-iT OliGreen (Life Technologies) assay was used to determine the number of duplexes per nanoparticle. siRNA duplex stability on the SNA over 75 d was characterized using urea dehybridization and centrifugation protocols (details in *SI Text, SNA Synthesis and Characterization*). GM3S expression was analyzed by RT-PCR and Western blotting after immortalized mKCs were treated with GM3S SNAs (details in *SI Text, In Vitro Studies*, and Fig. S1). GM3 expression was screened by confocal immunofluorescence with anti-GM3 antibody (Seikagaku Biobusiness Corp.). Toxicity of lipofected siRNA and SNAs was assessed by trypan blue exclusion cell viability assay (Sigma).

In Vitro Proliferation and Migration Assays. Primary mKCs were plated in 96-well plates (2×10^3 cells per well) in complete CnT07 serum-free media (Zen-Bio) with and without D-glucose supplement (18 mM final concentration).

Cells were treated with 2 nM GM3S or NS SNA, and proliferation was assessed daily for 5 d using a water-soluble tetrazolium assay as per the manufacturer's instructions (Clontech). For the migration assay, KCs were densely plated after treatment with 2 nM GM3S or NS SNA for 48 h in complete serum-free medium. Mitomycin C (5 μg/mL) was used to incubate cells for 1 h before a 500-μm-width scratch was made. Wound closure was serially imaged on an inverted light microscope (Nikon) at baseline and after 48 and 60 h postscratching.

In Vivo Wound-Healing Model. All mouse studies were approved by the Northwestern University (NU) Animal Care and Use Committee. Male C57BL/6 mice (Jackson Laboratory) were fed a high-fat diet [60% fat (percentage by total weight content); Harlan Teklad] ad libitum for at least 12 wk beginning at 6 wk of age, at which point the mice were obese (average weight of 43 g) and diabetic, which was assessed by glucose tolerance testing at least 1–2 wk before experimentation as previously described (4). Two full-thickness, circular, 6-mm-diameter wounds were made on the dorsal surface of each mouse, and silicone splints were placed around each wound (*SI Text, In Vivo Studies*).

Immunoblotting, RT-PCR, and 5′-RLM-RACE Analyses. Immunoblotting and RT-PCR analyses were performed as previously described (4, 17) (*SI Text, In Vivo Studies*); 5′-RLM-RACE analysis was performed using a kit from Invitrogen using the manufacturer's protocols (*SI Text, In Vivo Studies*).

Clinical, Histological, and Immunohistochemical Analyses. Wounds were gently wiped with water to remove unpenetrated SNAs and debris, and photographs were taken at wounding and every 48 h thereafter using photography standardized for distance and lighting. Wounds were dissected to muscle and embedded in paraffin for routine histological and immunohistochemical analyses. All histological and immunohistochemical preparations were performed at NU's Skin Disease Research Center Morphology and Phenotyping Core or Mouse Histology and Phenotyping Laboratory. H&E-stained 4-μm tissue sections were imaged using a TissueFAXS System (TissueGnostics; NU Cell Imaging Facility). The epidermal gap was defined as the maximal gap between the leading edges of epidermal migration, with an epidermal gap of zero signifying completely reepithelialization. The granulation tissue was defined by the vascular-enriched wound tissue between epidermis and fat/muscle tissue. All images were analyzed by two trained and blinded observers (details in *SI Text, In Vivo Studies*).

SNA Biodistribution. To determine SNA uptake into organs after topical delivery, kidneys, liver, lungs, lymph nodes, spleen, and total wounded skin area were harvested 12 d after wounding, and SNA gold content was quantified by inductively coupled plasma MS analysis (*SI Text, In Vivo Studies*). The nanoparticle concentration in each organ was reported as the percentage of the topically applied SNA per organ normalized to organ weight (Fig. S7).

Statistical Analyses. The Student's *t* test was used to assess significance of in vitro study data, and multifactor ANOVA was performed to assess the mouse studies with posthoc comparisons for individual comparisons using the Student's *t* test. $P < 0.05$ was considered significant for all analyses.

ACKNOWLEDGMENTS. We thank Ms. Harshitha Mannam and Ms. Lindsey Wold for their help in quantifying granulation tissue and p–insulin-like growth factor-1 receptor in histological sections of wounds and Dr. Timothy Merkel, Suguna Narayan, and William Briley for helpful discussions. This research was supported by National Institute of Arthritis and Musculoskeletal and Skin Diseases (NIAMS) Grant R21AR062898 and Center for Cancer Nanotechnology Excellence Initiative of the NIH/National Cancer Institute (NCI) Grant U54 CA151880. P.S.R. is supported by National Science Foundation Graduate Research Fellowship Grant DGE-1324585. We acknowledge core resources provided by Northwestern University (NU) Skin Disease Research Center NIAMS Grant P30AR057216, NU Mouse Histology and Phenotyping Laboratory NCI Cancer Center Support Grant (CCSG) P30CA060553, and NU Cell Imaging Facility NCI CCSG P30CA060553.

1. Sen CK, et al. (2009) Human skin wounds: A major and snowballing threat to public health and the economy. *Wound Repair Regen* 17(6):763–771.
2. Sun BK, Siprashvili Z, Khavari PA (2014) Advances in skin grafting and treatment of cutaneous wounds. *Science* 346(6212):941–945.
3. Anonymous (2014) *Statistics About Diabetes. National Diabetes Statistics Report*. Available at www.diabetes.org/diabetes-basics/statistics/. Accessed January 4, 2014.
4. Wang XQ, et al. (2014) Ganglioside GM3 depletion reverses impaired wound healing in diabetic mice by activating IGF-1 and insulin receptors. *J Invest Dermatol* 134(5):1446–1455.
5. Yamashita T, et al. (2003) Enhanced insulin sensitivity in mice lacking ganglioside GM3. *Proc Natl Acad Sci USA* 100(6):3445–3449.
6. Hotamisligil GS, Murray DL, Choy LN, Spiegelman BM (1994) Tumor necrosis factor alpha inhibits signaling from the insulin receptor. *Proc Natl Acad Sci USA* 91(11):4854–4858.
7. Tagami S, et al. (2002) Ganglioside GM3 participates in the pathological conditions of insulin resistance. *J Biol Chem* 277(5):3085–3092.
8. Memon RA, et al. (1999) Regulation of glycosphingolipid metabolism in liver during the acute phase response. *J Biol Chem* 274(28):19707–19713.
9. Zhao H, et al. (2007) Inhibiting glycosphingolipid synthesis improves glycemic control and insulin sensitivity in animal models of type 2 diabetes. *Diabetes* 56(5):1210–1218.
10. Aerts JM, et al. (2007) Pharmacological inhibition of glucosylceramide synthase enhances insulin sensitivity. *Diabetes* 56(5):1341–1349.
11. Yew NS, et al. (2010) Increased hepatic insulin action in diet-induced obese mice following inhibition of glucosylceramide synthase. *PLoS ONE* 5(6):e11239.
12. Zhao H, et al. (2009) Inhibiting glycosphingolipid synthesis ameliorates hepatic steatosis in obese mice. *Hepatology* 50(1):85–93.
13. Rosi NL, et al. (2006) Oligonucleotide-modified gold nanoparticles for intracellular gene regulation. *Science* 312(5776):1027–1030.
14. Giljohann DA, Seferos DS, Prigodich AE, Patel PC, Mirkin CA (2009) Gene regulation with polyvalent siRNA-nanoparticle conjugates. *J Am Chem Soc* 131(6):2072–2073.
15. Seferos DS, Prigodich AE, Giljohann DA, Patel PC, Mirkin CA (2009) Polyvalent DNA nanoparticle conjugates stabilize nucleic acids. *Nano Lett* 9(1):308–311.
16. Choi CHJ, Hao L, Narayan SP, Auyeung E, Mirkin CA (2013) Mechanism for the endocytosis of spherical nucleic acid nanoparticle conjugates. *Proc Natl Acad Sci USA* 110(19):7625–7630.
17. Zheng D, et al. (2012) Topical delivery of siRNA-based spherical nucleic acid nanoparticle conjugates for gene regulation. *Proc Natl Acad Sci USA* 109(30):11975–11980.
18. Jensen SA, et al. (2013) Spherical nucleic acid nanoparticle conjugates as an RNAi-based therapy for glioblastoma. *Sci Transl Med* 5(209):209ra152.
19. Lai-Cheong JE, McGrath JA (2006) Advances in understanding the genetic basis of inherited single gene skin barrier disorders: New clues to key genes that may be involved in the pathogenesis of atopic dermatitis. *An Bras Dermatol* 81(6):567–571.
20. Wang XQ, Sun P, Paller AS (2003) Ganglioside GM3 blocks the activation of epidermal growth factor receptor induced by integrin at specific tyrosine sites. *J Biol Chem* 278(49):48770–48778.
21. Seitz O, et al. (2010) Wound healing in mice with high-fat diet- or ob gene-induced diabetes-obesity syndromes: A comparative study. *Exp Diabetes Res* 2010:476969.
22. Galiano RD, Michaels J, 5th, Dobryansky M, Levine JP, Gurtner GC (2004) Quantitative and reproducible murine model of excisional wound healing. *Wound Repair Regen* 12(4):485–492.
23. Vicentini FT, et al. (2013) Delivery systems and local administration routes for therapeutic siRNA. *Pharm Res* 30(4):915–931.
24. Chen M, et al. (2014) Topical delivery of siRNA into skin using SPACE-peptide carriers. *J Control Release* 179:33–41.
25. Yamada T, et al. (2013) Wnt/β-catenin and kit signaling sequentially regulate melanocyte stem cell differentiation in UVB-induced epidermal pigmentation. *J Invest Dermatol* 133(12):2753–2762.
26. Lin CM, et al. (2012) A simple, noninvasive and efficient method for transdermal delivery of siRNA. *Arch Dermatol Res* 304(2):139–144.
27. Hsu T, Mitragotri S (2011) Delivery of siRNA and other macromolecules into skin and cells using a peptide enhancer. *Proc Natl Acad Sci USA* 108(38):15816–15821.
28. Uchida T, Kanazawa T, Kawai M, Takashima Y, Okada H (2011) Therapeutic effects on atopic dermatitis by anti-RelA short interfering RNA combined with functional peptides Tat and AT1002. *J Pharmacol Exp Ther* 338(2):443–450.
29. Yi X, et al. (2011) MITF-siRNA formulation is a safe and effective therapy for human melasma. *Mol Ther* 19(2):362–371.
30. Jacobson GB, et al. (2010) Biodegradable nanoparticles with sustained release of functional siRNA in skin. *J Pharm Sci* 99(10):4261–4266.
31. Chen Y, Bathula SR, Yang Q, Huang L (2010) Targeted nanoparticles deliver siRNA to melanoma. *J Invest Dermatol* 130(12):2790–2798.
32. Li Y, Fan J, Chen M, Li W, Woodley DT (2006) Transforming growth factor-alpha: A major human serum factor that promotes human keratinocyte migration. *J Invest Dermatol* 126(9):2096–2105.
33. Ando Y, Jensen PJ (1993) Epidermal growth factor and insulin-like growth factor I enhance keratinocyte migration. *J Invest Dermatol* 100(5):633–639.
34. Stachelscheid H, et al. (2008) Epidermal insulin/IGF-1 signalling control interfollicular morphogenesis and proliferative potential through Rac activation. *EMBO J* 27(15):2091–2101.
35. Haase I, Evans R, Pofahl R, Watt FM (2003) Regulation of keratinocyte shape, migration and wound epithelialization by IGF-1- and EGF-dependent signalling pathways. *J Cell Sci* 116(Pt 15):3227–3238.
36. Chung T-W, et al. (2009) Ganglioside GM3 inhibits VEGF/VEGFR-2-mediated angiogenesis: Direct interaction of GM3 with VEGFR-2. *Glycobiology* 19(3):229–239.
37. Nguyen PD, et al. (2010) Improved diabetic wound healing through topical silencing of p53 is associated with augmented vasculogenic mediators. *Wound Repair Regen* 18(6):553–559.
38. Courties G, et al. (2014) In vivo silencing of the transcription factor IRF5 reprograms the macrophage phenotype and improves infarct healing. *J Am Coll Cardiol* 63(15):1556–1566.